ATMOSPHERIC SCIENCE LETTERS
Atmos. Sci. Let. **17**: 280–285 (2016)
Published online 27 March 2016 in Wiley Online Library
(wileyonlinelibrary.com) **DOI:** 10.1002/asl.656

RMetS
Royal Meteorological Society

Recent ENSO–PDO precipitation relationships in the Mediterranean California border region

Edgar G. Pavia,[1,*] Federico Graef[1,2] and Ramón Fuentes-Franco[2]

[1] *Centro de Investigación Científica y de Educación Superior de Ensenada (CICESE), Ensenada, Mexico*
[2] *The Abdus Salam International Centre for Theoretical Physics (ICTP), Trieste, Italy*

**Correspondence to: E. G. Pavia, Centro de Investigación Científica y de Educación Superior de Ensenada (CICESE), PO Box 434844, San Diego, CA 92143-4844, USA. E-mail: epavia@cicese.mx*

Received: 8 November 2015
Revised: 31 January 2016
Accepted: 10 February 2016

Abstract

The Mediterranean California Border Region (MCBR) rainfall's relationship with El Niño-Southern Oscillation (ENSO) and the Pacific Decadal Oscillation (PDO) is reexamined for the period 1951–2014. When stratifying data by ENSO events we found that strong events of either sign yield the highest ENSO–rainfall correlation; but when the stratification was done by rainfall the wet seasons yield the highest ENSO–rainfall correlation. Most strong ENSO events have the same sign as PDO; but the ENSO–rainfall correlation for all ENSO–PDO same-sign events is almost undistinguishable from the full-record's correlation. Timewise stratification shows that 30-year climatological values (MCBR precipitation, PDO and ENSO) and ENSO–rainfall correlations have decreased in recent years.

Keywords: **Baja California rainfall; California rainfall; ENSO PDO rainfall relationships**

1. Introduction

The influence of the El Niño-Southern Oscillation (ENSO) phenomenon on the rainfall of southern California is well-known (e.g. Schonher and Nicholson, 1989; Fierro, 2014). The situation is similar in northwestern Baja California as rainfall regimes are comparable on both sides of the United States–Mexico border (Pavia and Graef, 2002). The southwestern California-northwestern Baja California region is part of the Mediterranean Californias (Pavia and Badan, 1998), because it is characterized by dry summers and wet winters, with usually wetter winters during warm ENSO (El Niño) events than during cool ENSO (La Niña) events; therefore, this region hereinafter shall be referred to as the Mediterranean California Border Region (MCBR). Furthermore decadal variability (e.g. Pacific Decadal Oscillation, PDO) is known to modulate the ENSO–rainfall relationship in this region in a constructive interference way (Gershunov and Barnett, 1998; Gershunov and Cayan, 2003; Pavia *et al.*, 2006). However in the last decade the ENSO–rainfall relationship in the MCBR has weakened, for example after the last 1997–1998 strong El Niño wet year, the only two recent wet seasons were the 2004–2005 (a neutral event) and the 2010–2011 La Niña. Climatologically this resulted in a reduction of both: 30-year ENSO–rainfall correlations and 30-year regional precipitation climatological values; the latter coinciding with a similar decline in ENSO and PDO climatologies. Therefore the study of these circumstances is of utmost importance for the MCBR, where several major cities are located and where precipitation averages only around 240 mm year^{-1} (see Figure 1). Within the MCBR the situation is even more critical for Baja California than California, because the former lacks the level of hydraulic infrastructure that the latter possesses (MacDonald, 2007). Elsewhere variations in ENSO–rainfall and ENSO–PDO–rainfall relationships have been noted as well (e.g. Rocha, 1999; Krishna Kumar *et al.*, 1999; McCabe and Dettinger, 1999; Chang *et al.*, 2001; Cai *et al.*, 2001; Sarkar *et al.*, 2004; Gao *et al.*, 2006; Zubair and Ropelewski, 2006; Kucharski *et al.*, 2007); thus in this paper we study the changes in ENSO, PDO and rainfall in the MCBR (Figure 1), focusing on the recent 1951–2014 period. Our goal is not to scrutinize single or particular events, but to examine different subsets of our record (stratified in different ways) searching for rather general relationships of the MCBR rainfall with ENSO and PDO.

2. Data and methods

We construct ENSO, PDO and MCBR rainfall indices to obtain baseline correlations among them (for the entire period) and subset correlations for different stratifications (by index values and timewise). We also compute 30-year climatological values for these three variables plus 30-year ENSO–rainfall and PDO′–PDO correlations; where PDO′ is an 'ENSO-forced' model (see Newman *et al.*, 2003; Pavia, 2009). Finally we construct global maps of SST–ENSO and SST–regional precipitation correlation patterns for different periods to substantiate our results.

2.1. Original data

For ENSO we select the monthly El Niño 3.4 index from NOAA's Earth System Research Laboratory/Physical

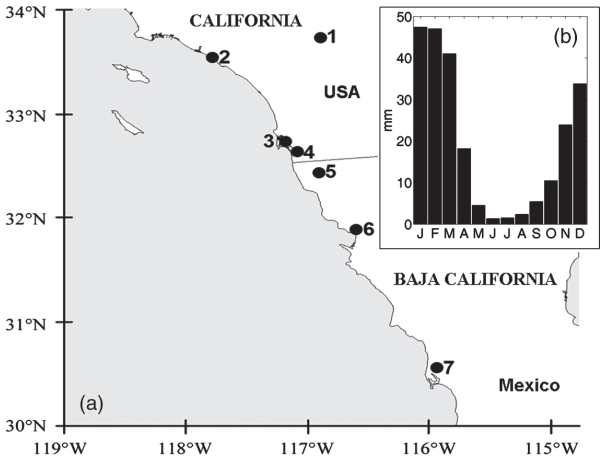

Figure 1. (a) The region of study. Numbers besides a solid circle indicate the stations considered: 1. Hemet, 2. Laguna Beach, 3. San Diego, 4. Chula Vista, 5. Tijuana, 6. Ensenada, 7. San Quintin. (b) Bars indicate the 1951–2014 monthly climatological values of precipitation averaged over the seven stations (annual mean 237 mm year^{-1}).

Sciences Division (ESRL/PSD) because the region of the El Niño 3.4 index is closely related to extra-tropical teleconnections; however, using other ENSO indices yields similar results. For decadal variability we select the PDO index (obtained from the University of Washington's Joint Institute for the Study of the Atmosphere and Ocean). For regional rainfall we select the monthly precipitation data from seven stations: Hemet (PHE), Laguna Beach (PLB), San Diego (PSD) and Chula Vista (PCV), California, obtained from the National Weather Service (NWS) among many others, and from Tijuana (PTJ), Ensenada (PEN) and San Quintin (PSQ), Baja California, obtained from the Mexican Water Authority (CNA) (see Figure 1). We also use global SST data from the Hadley Center (HadISST, Rayner *et al.*, 2003), and gridded precipitation data from Livneh *et al.* (2013) within the region between 115° and 120°W and 30° and 34.5°N to perform further correlation analyses to verify our results. A preliminary analysis of the seven stations and gridded precipitation data gave comparable results; thus the stations dataset is considered typical of MCBR precipitation.

2.2. Data preparation and correlation analyses

We begin by calculating the average of annual total (July to June) precipitation of the seven stations: PHE, PLB, PSD, PCV, PTJ, PEN and PSQ; we consider the standardized average to be representative of our region's rainfall and call it CPI (CPI and a similar index calculated from the gridded data of Livneh *et al.* (2013) are correlated above 0.9). Similarly for the ENSO and PDO indices we use annual averages of the El Niño 3.4 index and the PDO index (also July to June), and call them ENI and PDI (Figure 2). The correlations of ENI and PDI with CPI are performed for the entire 63-year series, as a first assessment of their relationship, and for 30-year running periods. The ENSO–PDO relationship

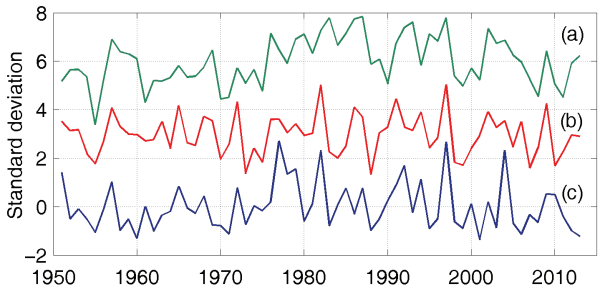

Figure 2. The constructed annual indices: (a) PDO (PDI + 6), (b) ENSO (ENI + 3), (c) MCBR precipitation (CPI).

is assessed thru the use of a model: PDI′ = f(PDI, ENI). We then stratify data by index value to obtain subset correlations; similarly we stratify data timewise by periods and by seasons and calculate climatological values in addition to subset correlations. Finally four series of global SST–ENSO–rainfall spatial correlation maps (1951–1981, 1965–1995, 1983–2013 and 1951–1965 plus 1999–2014) are calculated to examine the details of our results. We selected the mentioned periods in order to show the differences in SST–regional precipitation and SST–ENSO correlation patterns depending on the dominant ENSO phase in each period. The period 1983–2013 includes the two El Niño events with the overall highest amplitude (1983 and 1998), while the 1951–1965 plus 1999–2014 combined-period excludes the four strongest ENSO events during winter (1965–1966, 1972–1973, 1982–1983 and 1997–1998) (see Figure 3).

3. Results

3.1. ENI–CPI correlation

The baseline correlation for our entire record is $R_{all} = 0.58$; thus only about one third of recent MCBR rainfall variability may be explained by ENSO.

3.1.1. Stratification by ENSO events

To further investigate the correlation between ENI and CPI, we stratified the ENI data into strong ENSO events ($|ENI| > 0.8$) and neutral events ($-0.8 \leq ENI \leq 0.8$). This yields 25 strong ENSO (12 positive) and 38 neutral ENSO events. The correlation $R_{strong} = 0.83$, is statistically significant as the probability of getting a correlation as large as the observed value by random chance is 10^{-7}, lower and upper bounds for a 95% confidence interval for R_{strong} are [0.64, 0.92]. All but 1 year out of 12 with strong positive ENSO have CPI > 0; that is, rain above the mean. Also all but 2 years out of 13 with strong negative ENSO (ENI < −0.8) have CPI < 0; that is, rain below the mean (see Figure 4). This is the most robust result we could find in these data. With the definition more commonly used in the literature: $|ENI| > 1.0$, we obtained 20 strong and 43 neutral

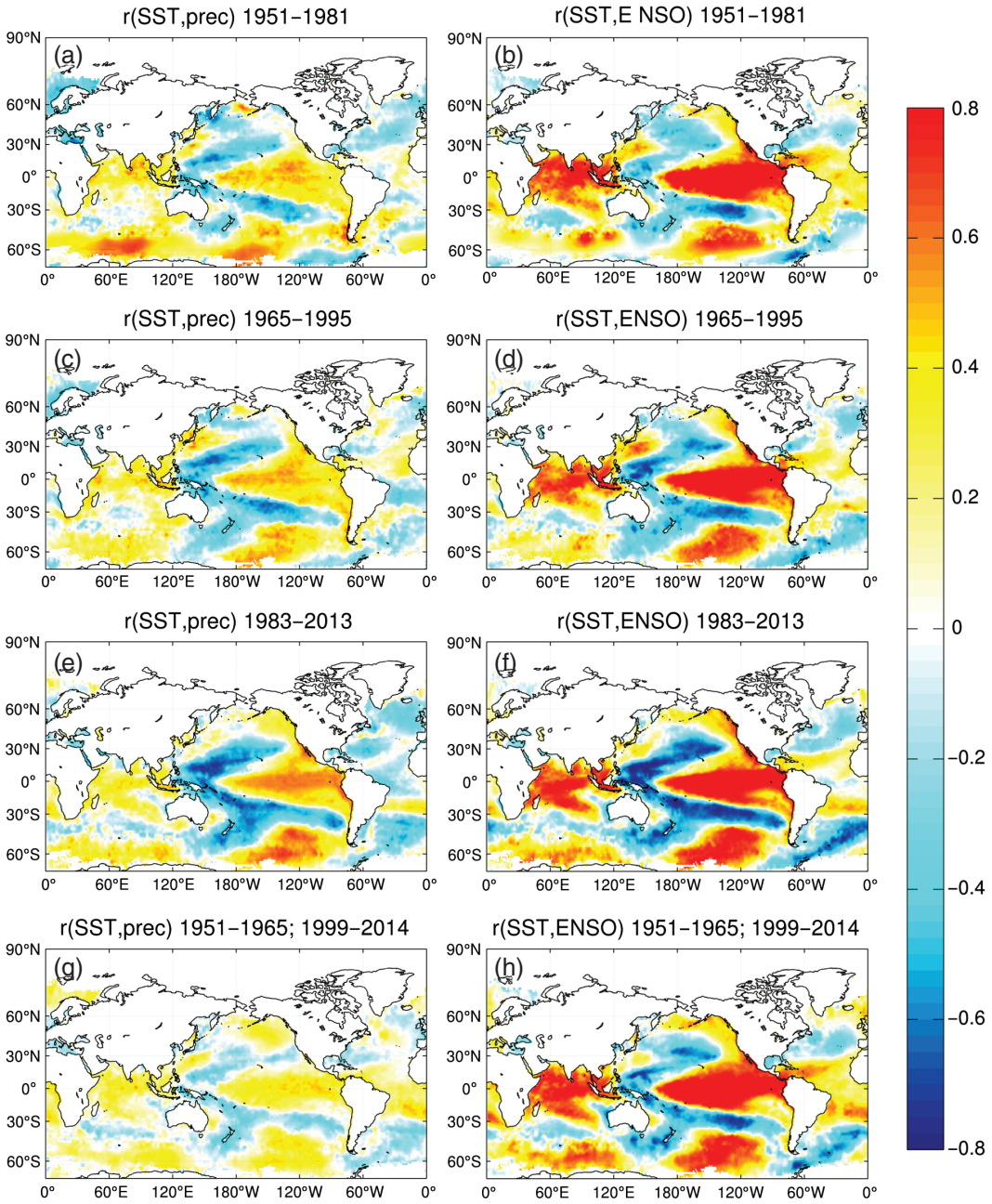

Figure 3. (a) Correlations (value indicated by the color bar) between MCBR annual rainfall and global SST for the period 1951–1981. (b) Correlations between ENSO3.4 index and global SST for the period 1951–1981. (c) and (d) Same as (a) and (b), respectively, but for the 1965–1995 period. (e) and (f) Same as (a) and (b) respectively but for the 1983–2013 period. (g) and (h) Same as (a) and (b) but for the 1951–1965 and 1999–2014 period.

events, and it yields $R_{\text{strong}} = 0.82$, $R_{\text{neutral}} = 0.41$, correlations which are statistically indistinguishable from those obtained using $|\text{ENI}| > 0.8$.

3.1.2. Stratification by regional rainfall events

Similarly when we stratified by wet ($\text{CPI} > \varepsilon$), dry ($\text{CPI} < -\varepsilon$) and neither ($-\varepsilon \leq \text{CPI} \leq \varepsilon$) events (using different values for ε, from 0.5 to 1.0), the correlations were always higher for R_{wet} (~0.5, and significant) than for R_{dry} (~0.0, and non-significant). For R_{neither} we also found values comparable with R_{wet}, but only marginally significant.

3.1.3. Seasonal analysis

We also averaged monthly El Niño 3.4 Index data (ENSO) by season; that is, winter: January, February and March; spring: April, May and June; summer: July, August and September; autumn: October, November and December. For precipitation data (RAIN) we calculated totals for winter and autumn. After an extensive statistical analysis we found that seasonal correlations are in all cases lower than $R_{\text{all}} = 0.58$. The highest correlation found was $R(\text{ENSO}_{\text{winter}}, \text{RAIN}_{\text{winter}}) = 0.55$; when using ENSO lagged data we found that ENSO's previous year gives $R(\text{ENSO}_{\text{autumn }(n-1)}, \text{RAIN}_{\text{winter}}) = 0.50$. We did not find

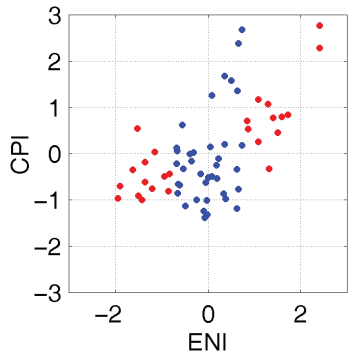

Figure 4. Stratification by ENSO strength: strong ENSO (|ENI| > 0.8) and neutral ENSO (−0.8 ≤ ENI ≤ 0.8), red and blue, respectively.

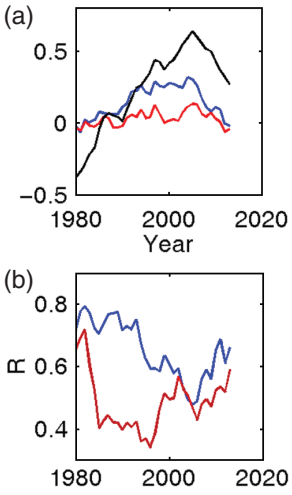

Figure 5. (a) Running 30-year climatologies from 1951–1980 to 1984–2013. (Recall that 2013 means July 2013 to June 2014), PDI (in black), CPI (in blue), ENI (in red). (b) Running 30-year correlations from 1951–1980 to 1984–2013, *R*(PDI′, PDI) (in blue), *R*(ENSO, PDO) (in red).

correlations $\text{RAIN}_{\text{winter}}$ (or $\text{RAIN}_{\text{autumn}}$) with any other ENSO season higher than 0.50. In general correlations increase as the ENSO season gets closer to $\text{RAIN}_{\text{winter}}$.

3.1.4. SST–ENSO–rainfall correlation maps

We correlated all regional seasonal winter precipitation with the gridded global SST at all grid points (Figure 3). Similarly we correlated the ENSO index with the gridded global SST. All ENSO–SST correlation maps (Figure 3(b), (d), (f), (h)) show similar patterns among them for positive correlations in the Pacific, in contrast with the precipitation–SST correlation maps. The 1983–2013 period shows the highest correlation patterns (Figure 3(e)), it includes the strongest El Niño events (1983 and 1998), and furthermore this period exhibits the greatest similarity between ENSO–SST correlation (Figure 3(f)) and precipitation–SST correlation (Figure 3(e)). The period with the lowest correlation patterns is 1951–1965 plus 1999–2014, which excludes the four strongest ENSO events during the wintertime within our record: 1965–1966, 1972–1973, 1982–1983 and 1997–1998 (Figure 3(g)), and which also shows the greatest difference with the ENSO–SST correlation patterns (Figure 3(h)).

3.2. The role of the PDO

3.2.1. ENI–CPI correlation

Considering the stratification done in Section 3.1.1 we found that PDI and ENI have the same sign in 76% of strong ENSO events; but the ENI–CPI correlation for all ENSO–PDO same-sign events is $R = 0.62$.

To further investigate the constructive interference of Gershunov *et al.* (1999) we varied the criterion parameter (φ) that we used to stratify strong and neutral ENSO years from 0.5 to 1.0 and also stratified the years as follows:

(i) PDI ≥ 0 and ENI ≥ φ, (positive phase of PDO and strong El Niño).
(ii) PDI < 0 y ENI < $-\varphi$ (negative phase of PDO and strong La Niña).
(iii) (i) and (ii).

For example, for $\varphi = 0.5$ (0.8) we get 13 (8), 16 (11) and 29 (19) years for cases (i), (ii) and (iii), respectively. Comparing the corresponding correlation matrices, the correlations (ENI, PDI) and (PDI, CPI) are higher in general (some statistically significantly) in case (iii) than in case (i) but more so than in case (ii). None of the correlations in case ii) is significant and the highest correlation is $R(\text{ENI, PDI}) = -0.54$ for $\varphi = 1.0$, with 95% CI being [−0.89, 0.19]. In contrast, all correlations in case iii) are significant. With respect to *R*(ENI, CPI), it increases from 0.32 for $\varphi = 0.5$ to 0.90 for $\varphi = 1.0$ in case (i), and from 0.72 to 0.82 (not a significant increase) in case (ii); there is also an increase in case (iii), with respect to (i) and (ii), but only for values of $\varphi = 0.5$, 0.6 and 0.7. These results are in line with those found in Pavia *et al.* (2006): El Niño and the positive phase of PDO show constructive interference, but La Niña and a negative phase of PDO do not. Correlations for negative PDI and negative ENI (23 years) are low and non-significant, compared with the cases positive PDI and positive ENI (20 years).

3.2.2. 30-year analysis

The most notorious feature here is that climatological values have decreased most recently: precipitation, since the 1975–2004 period, PDO since the 1976–2005 period, and ENSO since the 1977–2006 period; while the ENI–CPI correlations ($R_{1957-1986} = 0.53 < R(\text{ENI, CPI}) < R_{1970-1999} = 0.73$) have experienced a similar decrease, that is $R_{1984-2013} = 0.54$ (see Figure 5(a)). This may be related to the fact that within our period there was a low-frequency positive PDO phase during the last quarter of the 20th century. There is also tree-ring evidence that during this period the region was unusually (in a 1000-year record) wet (Swetnam and Betancourt, 1998).

3.2.3. PDO ENSO-dependency

In this case we investigated the variability of the ENSO–PDO relationship within our period thru the use of a 'forced' model: $\mathrm{PDI}_n' \sim \alpha \times \mathrm{PDI}_{n-1} + \beta \times \mathrm{ENI}_n$ (see Pavia, 2009) for the entire record and for 30-year running periods. For the entire record we found $R(\mathrm{PDI}', \mathrm{PDI})_{\mathrm{all}} = 0.70$, and for the running correlations: $R_{1976-2005} = 0.48 < R(\mathrm{PDI}', \mathrm{PDI}) < R_{1953-1982} = 0.79$ (see Figure 5(b)).

4. Discussion and conclusions

The ENSO influence and the PDO–ENSO constructive interference on annual MCBR precipitation have been confirmed for the period 1951–2014. However the latter is clearer for the case of strong ENSO events of either sign (in 19 out of 25 events ENI and PDI have the same sign and the ENI–CPI correlation is $R_{\mathrm{strong}} = 0.83$) than for any other case: neutral, strong-positive, strong-negative, etc. (see Figure 4). Nevertheless the ENI–CPI correlation for all ENI–PDI same-sign events ($R_{\mathrm{same\text{-}sign}} = 0.62$) is statistically undistinguishable from the baseline correlation ($R_{\mathrm{all}} = 0.58$). That is, apart from the strong ENSO case, only about one third of regional annual rainfall variability may be explained by ENSO. Also in this period dry years are significantly less related to ENSO ($R_{\mathrm{dry}} = -0.04$) compared with wet years ($R_{\mathrm{wet}} = 0.47$), and 85% (92%) of strong negative (positive) ENSO events correspond to years with precipitation below (above) the mean; this is the opposite of what has been suggested: i.e. that La Niña is more consistently and predictably related to dry winters in the region than El Niño is related to wet winters (e.g. Gershunov and Barnett, 1998, Gershunov and Cayan, 2003). Seasonally winter precipitation is better related to winter ENSO than to other season's ENSO values; however, the heavy 1977–1978 regional precipitation (see Figure 2) was not related to a strong positive ENSO event, but rather to a climate shift in the Pacific Ocean (Miller *et al.*, 1994), neither does the recent MCBR drought seem to be associated with La Niña (Seager *et al.*, 2014): the 2010–2011 La Niña was a wet year. This explains the recent decrease in 30-year ENI-CPI correlations (Section 3.2.2), which is almost concurrent with the recent decrease in 30-year climatological values for PDI, ENI and CPI (see Figure 5(a)). This may be related to a somewhat weaken influence of ENSO on the PDO (Figure 5(b)) during the peak of the 30-year PDI value (Figure 5(a)), or perhaps exceptional years, such as 1977–1978 and 2010–2011, weaken the ENSO–MCBR rainfall relationship in general compared with the only strong ENSO case. Furthermore SST–ENSO-regional precipitation maps show that MCBR annual rainfall is clearly influenced by ENSO during periods with strong warm events, as revealed by conspicuous positive correlation patterns (see Figure 3). That is, in the absence of strong El Niño events regional precipitation is not well correlated to ENSO, and frequent rainy seasons usually concur with repeated warm ENSO events, but several years of low precipitation do not always relate with frequent cool ENSO events. This is in line with recent findings, for example: of the last three dry seasons, only the 2011–2012 season was found to be a response to La Niña, whereas the 2012–2013 and 2013–2014 seasons were related to a warm tropical west Pacific sea surface temperature anomaly (Seager *et al.*, 2014). Consequently for the last 60 years or so wet (dry) periods correspond to higher (lower) ENSO–regional rainfall correlations.

Therefore in general, that is irrespective of particular events, strong ENSO events of either sign are good predictors of rainfall in the Mediterranean Californias: strong positive (negative) events implying wet (dry) years; but otherwise ENSO (in general: that is irrespective of particular years) is not a good predictor for rainfall in our region. Similarly constructive interference is only effective for strong ENSO events; otherwise the general coincidence of ENI and PDI signs impacts ENI–CPI correlations very slightly. For dry years the correlations (ENI, CPI) and (PDI, CPI) were found to be negative or not significantly different from zero.

In the last 15 years, besides the 2010 El Niño and the 2011 La Niña, which did not result in expected precipitation anomalies, the lack of strong ENSO events may explain why ENSO has not been a good predictor for MCBR precipitation recently. It can also be that what we call the past positive phase of the PDO during the last quarter of the 20th century was an exceptional period, as shown by a 1000-year tree-ring record (Swetnam and Betancourt, 1998), and the last 15 years is just a return to the normal conditions, similar to the pre-1977 situation.

Finally considering the 2015 El Niño which is expected to influence weather and climate patterns for the 2015–2016 winter: timewise this event is occurring during a dry and lower ENI–CPI correlation period; nevertheless our analysis of ENSO strength stratification indicates that strong events such as the 2015 El Niño are very likely to correspond to a very rainy season in our region. The October 2015 US Winter Outlook, issued by NOAA's Climate Prediction Center (http://www.noaanews.noaa.gov/stories2015/), indicates wetter than average conditions for southwestern California and other southern US states. Also the Mexican Meteorological Service is forecasting precipitations above normal in northwestern Baja California in particular and in northwestern Mexico in general. These statements are both in line with our ENSO-stratification results, with the caveat of our timewise climatological results indicating the recent weakening of the ENSO-rainfall relationship in our region.

Acknowledgements

This work was funded by CONACYT (Mexico). We thank Sasha Gershunov for many insightful suggestions and several brief, but fruitful discussions.

References

Cai W, Whetton PH, Pittock AB. 2001. Fluctuations of the relationship between ENSO and northeast Australia rainfall. *Climate Dynamics* **17**: 421–432.

Chang CP, Harr P, Ju J. 2001. Possible roles of Atlantic circulations on the weakening Indian monsoon rainfall–ENSO relationship. *Journal of Climate* **14**: 2376–2380.

Fierro AO. 2014. Relationships between California rainfall variability and large-scale climate drivers. *International Journal of Climatolology* **34**: 3626–3640.

Gao H, Wang YG, He J. 2006. Weakening significance of ENSO as a predictor of summer precipitation in China. *Geophysical Research Letters* **33**: L09807, doi: 10.1029/2005GL025511.

Gershunov A, Barnett T. 1998. Interdecadal modulation of ENSO teleconnections. *Bulletin of the American Meteorological Society* **79**: 2715–2726.

Gershunov A, Cayan DR. 2003. Heavy daily precipitation frequency over the contiguous United States: sources of climatic variability and seasonal predictability. *Journal of Climate* **16**: 2752–2765.

Gershunov A, Barnett T, Cayan DR. 1999. North Pacific interdecadal oscillation seen as factor in ENSO-related North American climate anomalies. *Eos* **80**: 25–30.

Krishna Kumar K, Rajagopalan B, Cane MA. 1999. On the weakening relationship between the Indian monsoon and ENSO. *Science* **284**: 2156–2159.

Kucharski F, Bracco A, Yoo JH, Molteni F. 2007. Low-frequency variability of the Indian monsoon–ENSO relationship and the Tropical Atlantic: the "weakening" of the 1980s and 1990s. *Journal of Climate* **20**: 4255–4265.

Livneh B, Rosenberg EA, Lin C, Nijssen B, Mishra V, Andreadis KM, Maurer EP, Lettenmaier DP. 2013. A long-term hydrologically based dataset of land surface fluxes and states for the conterminous United States: update and extensions. *Journal of Climate* **26**: 9384–9392.

MacDonald GM. 2007. Severe and sustained drought in southern California and the West: present conditions and insights from the past on causes and impacts. *Quaternary International* **173–174**: 87–100.

McCabe GJ, Dettinger MD. 1999. Decadal variations in the strength of ENSO teleconnections with precipitation in the western United States. *International Journal of Climatology* **19**: 1399–1410.

Miller AJ, Cayan DR, Barnett TP, Graham NE, Oberhuber JM. 1994. The 1976–1977 climate shift of the Pacific Ocean. *Oceanography* **7**: 21–26.

Newman M, Compo GP, Alexander MA. 2003. ENSO-forced variability of the Pacific Decadal Oscillation. *Journal of Climate* **16**: 3853–3857.

Pavia EG. 2009. The relationship between Pacific Decadal and Southern Oscillations: implications for the climate of northwestern Baja California. *Geofísica Internacional* **48**: 385–389.

Pavia EG, Badan A. 1998. ENSO modulates rainfall in the Mediterranean Californias. *Geophysical Research Letters* **25**: 3855–3858.

Pavia EG, Graef F. 2002. The recent rainfall climatology of the Mediterranean Californias. *Journal of Climate* **15**: 2697–2701.

Pavia EG, Graef F, Reyes J. 2006. PDO-ENSO effects in the climate of Mexico. *Journal of Climate* **19**: 6433–6438.

Rayner NA, Parker DE, Horton EB, Folland CK, Alexander LV, Rowell DP, Kent EC, Kaplan A. 2003. Global analyses of sea surface temperature, sea ice, and night marine temperature since the late nineteenth century. *Journal of Geophysical Research* **108**(D14): 4407, doi: 10.1029/2002JD002670.

Rocha A. 1999. Low-frequency variability of seasonal rainfall over the Iberian Peninsula and ENSO. *International Journal of Climatolology* **19**: 889–901.

Sarkar S, Singh RP, Kafatos M. 2004. Further evidences for the weakening relationship of Indian rainfall and ENSO over India. *Geophysical Research Letters* **31**: L13209, doi: 10.1029/2004GL020259.

Schonher T, Nicholson SE. 1989. The relationship between California rainfall and ENSO events. *Journal of Climate* **2**: 1258–1269.

Seager R, Hoerling M, Schubert S, Wang H, Lyon B, Kumar A, Nakamura J, Henderson N. 2014. Causes and predictability of the 2011–2014 California drought. NOAA Drought Task Force Assement Report, NOAA, Silver Springs, MD, 42 pp. http://cpo.noaa.gov/MAPP/californiadroughtreport (accessed 8 November 2015).

Swetnam TW, Betancourt JL. 1998. Mesoscale disturbance and ecological response to decadal climatic variability in the American Southwest. *Journal of Climate* **11**: 3128–3147.

Zubair L, Ropelewski CF. 2006. The strengthening relationship between ENSO and northeast monsoon rainfall over Sri Lanka and Southern India. *Journal of Climate* **19**: 1567–1575.